

# Synthesis and Structural Characterization of Nano-sized Copper Tungstate Particles

Dragana J. Jovanović, Ivana Lj. Validžić, Miodrag Mitrić  
and Jovan M. Nedeljković\*

Vinča Institute of Nuclear Sciences, University of Belgrade, P.O. Box 522, 11001 Belgrade, Serbia

\* Corresponding author: E-mail: jovned@vinca.rs;  
phone: +(381)112438906; fax: +(381)112447382

Received: 09-03-2011

## Abstract

The nano-sized copper tungstate ( $\text{CuWO}_4$ ) was prepared by precipitation method in the presence of non-ionic copolymer surfactant (polyoxyethylene-polyoxypropylene block copolymer) and consequent annealing at low temperature ( $400\text{ }^\circ\text{C}$ ). The scanning electron microscopy (SEM) indicated formation of spherical  $\text{CuWO}_4$  particles in the size range from 10 to 90 nm. The thermogravimetric analysis was used to study dehydration processes. The X-ray diffraction analysis undoubtedly confirmed formation of triclinic  $\text{CuWO}_4$  and the refinement of the diffraction data showed that  $\text{CuWO}_4$  powder belongs to the distorted tungstate type of structure with space group P1. The structure of the  $\text{CuWO}_4$  can be described as infinite zigzag chains formed by edge-sharing alternating  $[\text{W}-\text{O}_6]$  and  $[\text{Cu}-\text{O}_6]$  octahedra. Indirect and direct band-gap energies of  $\text{CuWO}_4$  (2.3 and 3.5 eV, respectively) were determined using optical measurements.

**Keywords:** Copper tungstate; rietveld refinement; optical properties; block copolymer

## 1. Introduction

Transition metal tungstates are important family of inorganic materials that have a significant application potential in various fields.<sup>1</sup> Copper tungstate ( $\text{CuWO}_4$ ) is a well-known semiconductor with potential technological applications in scintillator detectors, laser hosts, photoanodes, optical fibers, etc.<sup>2–4</sup> Because of that, a wide range of studies such as photoelectrochemical investigations,<sup>5</sup> crystal growth,<sup>6,7</sup> electrical and electrochemical characterizations,<sup>8,9</sup> have been performed.

The most common techniques of forming  $\text{CuWO}_4$  are solid-state synthesis and liquid precipitation method. Solid-state synthesis of  $\text{CuWO}_4$  was achieved by heating an intimate mixture of equimolar proportions of CuO and  $\text{WO}_3$ ,<sup>10–12</sup> as well as  $\text{CuCl}_2$  and  $\text{Na}_2\text{WO}_4$  up to temperatures of  $850\text{ }^\circ\text{C}$ .<sup>7</sup> In solution, hydrated  $\text{CuWO}_4$  can be obtained by precipitation from corresponding salts, followed by annealing at temperatures up to  $800\text{ }^\circ\text{C}$  in order to obtain dehydrated crystalline  $\text{CuWO}_4$ .<sup>11–13</sup> It should be kept in mind that limiting temperature for synthesis of  $\text{CuWO}_4$  is  $935\text{ }^\circ\text{C}$ , i.e., starting temperature of thermal degradation of  $\text{CuWO}_4$ .<sup>14</sup>

In this paper, we used colloidal chemistry approach for preparation of hydrated  $\text{CuWO}_4$ . The stabilizer (poly-

oxyethylene-polyoxypropylene block copolymer) was present in solution in order to suppress particle's growth from nano to micron size domain. To the best of our knowledge, the soft solution methods that include the assistance of block copolymers have been applied only for other tungstates.<sup>15,16</sup> In the second step, annealing of hydrated  $\text{CuWO}_4$ , performed at  $400\text{ }^\circ\text{C}$ , led to the formation of crystalline  $\text{CuWO}_4$  powder. Structural and optical characterization of the  $\text{CuWO}_4$  powder was performed. Special attention was paid to the refinement of the crystal structure of the synthesized material.

## 2. Experimental

All chemicals ( $\text{Na}_2\text{WO}_4 \cdot 2\text{H}_2\text{O}$  (99% Riedel-de Haën),  $\text{CuCl}_2 \cdot 2\text{H}_2\text{O}$  (99% Merck), non-ionic copolymer surfactant Pluronic F68 (Polyoxyethylene-polyoxypropylene block copolymer,  $M_n \sim 8400$  (Aldrich)) were of the highest purity available and they were used without further purification.

Typically, 50 ml of 0.1 M  $\text{Na}_2\text{WO}_4 \cdot 2\text{H}_2\text{O}$  solution was mixed with 100 ml of copolymer solution (10 g/L). The pH of the solution was adjusted to 3 using concentrat-

ed HCl solution. Then, under vigorous stirring, 50 ml of 1.5 M  $\text{CuCl}_2 \cdot 2\text{H}_2\text{O}$  was added drop by drop. After that, the mixture was refluxed at 80 °C for 90 minutes. During the reflux, precipitation of hydrated  $\text{CuWO}_4$  took place. The hydrated  $\text{CuWO}_4$  was separated from solvent containing copolymer immediately after synthesis by using ultracentrifugation, then washed several times with ethanol and distilled water, and finally annealed at 400 °C for 48 hours in order to produce golden yellow crystalline  $\text{CuWO}_4$  powder.

It should be emphasized that identical synthetic procedure was used for a wide range of concentration ratio between reactants, but the pure  $\text{CuWO}_4$  phase was obtained in reaction with huge excess of  $\text{Cu}^{2+}$  ions compared to  $\text{WO}_4^{2-}$  ( $[\text{Cu}^{2+}]/[\text{WO}_4^{2-}] = 15$ ). The appearance of small amounts of impurities was noticed at equimolar concentrations of reactants or with slight excess of  $\text{Cu}^{2+}$  ions. Tungsten (VI) oxide was main impurity in the case of equimolar concentration of reactants, while with the increase of excess of  $\text{Cu}^{2+}$  ions sodium pyrotungstate appears to be a characteristic impurity.

The scanning electron microscopy (SEM) was performed using JEOL JSM-6460LV instrument (Tokyo, Japan). The  $\text{CuWO}_4$  sample was coated with thin layer of gold deposited by sputtering process.

Thermogravimetric (TG) and differential thermal analysis (DTA) measurements in air atmosphere were performed on dried, but not annealed  $\text{CuWO}_4$  sample using SETARAM SETSYS Evolution-1750 instrument (heating rate 10 °C  $\text{min}^{-1}$ ).

The X-ray Powder Diffraction (XRPD) patterns of investigated samples were obtained on a Philips PW-1050 automated diffractometer using Ni-filtered  $\text{CuK}_\alpha$  radiation (operated at 40 kV and 30 mA). A fixed 1° divergence and 0.1° receiving slits were used. Diffraction data for structural analysis were collected in the 2 $\theta$  range from 10 to 120°, with 0.02° steps and 12s exposition per step. Structural analysis was performed by using the KOALARIIE computing program based on the Rietveld full profile refinement method.<sup>17,18</sup> Samples for XRPD measurements were prepared using the standard protocol.<sup>19</sup>

The absorption spectra of dispersed  $\text{CuWO}_4$  particles in water were measured using Thermo Scientific Evolution 600 UV-Vis spectrophotometer.

### 3. Results and Discussion

Typical SEM image of the  $\text{CuWO}_4$  powder annealed at 400 °C for 48 hours is shown in Figure 1. The  $\text{CuWO}_4$  particles are mostly spherical in the size range from 10 to 90 nm. So far, synthesis of agglomerated micrometer in size copper tungstate particles was reported,<sup>11,13,20</sup> but, recently, Sen<sup>21</sup> and Montini<sup>22</sup> developed synthetic procedure for preparation of  $\text{CuWO}_4$  in nano- size regime. The polyoxyethylene-polyoxypropylene block copolymer have

been used to synthesize very small noble metal nanoparticles,<sup>23,24</sup> so that its presence on the particle surface prevented growth of  $\text{CuWO}_4$  from nano to micron size domain.

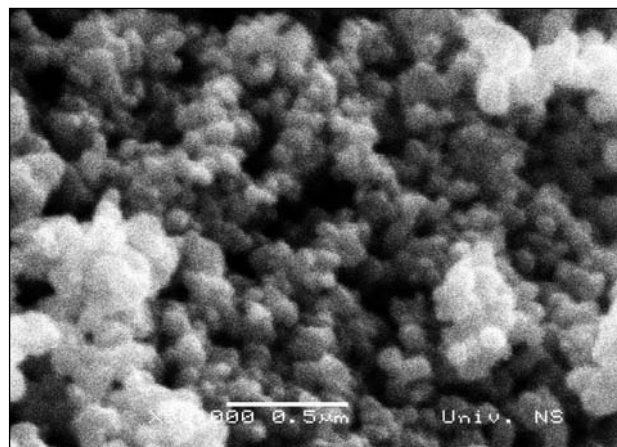
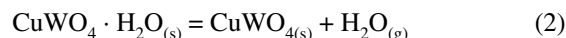


Figure 1. Typical SEM image of the  $\text{CuWO}_4$  particles.

Simultaneously measured, TG and DTA curves of dried, but not annealed,  $\text{CuWO}_4$  sample are shown in Figure 2. The total mass loss observed at temperatures higher than 400 °C is slightly smaller than 12%. At low temperatures (below 200 °C), the TG measurements revealed that the mass loss is little bit smaller than 10%. Assuming the following mechanism of dehydration process of  $\text{CuWO}_4 \cdot 2\text{H}_2\text{O}$ :



the observed mass loss corresponds well to the calculated value of the mass loss for dehydration of two water molecules (10.38%). The additional mass loss at higher tem-

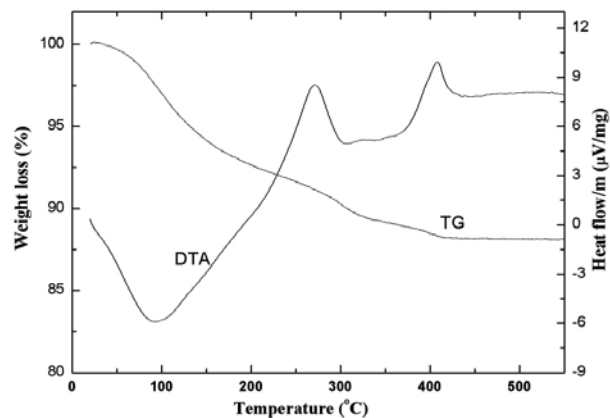


Figure 2. TG and DTA curves of copper tungstate dehydrate ( $\text{CuWO}_4 \cdot 2\text{H}_2\text{O}$ ).

peratures is most likely consequence of the oxidation in air traces of copolymer.

The DTA data are in agreement with TG measurements. Strong endothermic peak (around 100 °C) accompanied with shoulder (around 200 °C) corresponds to the dehydration of two water molecules, while two exothermic peaks at higher temperatures (around 250 and 400 °C) are most likely due to oxidation of copolymer traces.

Solid material obtained in the reflux reaction between sodium tungstate with huge excess of copper (II) chloride, in the presence of non-ionic copolymer surfactant (polyoxyethylene-polyoxypropylene block copolymer), thoroughly washed and annealed at 400 °C was analyzed using the XRPD measurements. It should be pointed out that annealing temperature is close to the proposed crystallization temperature of  $\text{CuWO}_4$  (410 °C).<sup>13</sup>

The starting parameters in the least-squares refinement were taken from Kihlberg<sup>25</sup> and the refinement of the diffraction data showed that  $\text{CuWO}_4$  powder belongs to the triclinic distorted wolframite type of structure. The intensity data were evaluated assuming the Voigt peak shape, and in this refinement 410 independent reflections were used. The refinement was done in the  $P\bar{1}$  space group in  $(\text{Cu}, \text{Zn})\text{WO}_4$  structural type where all ions occupy

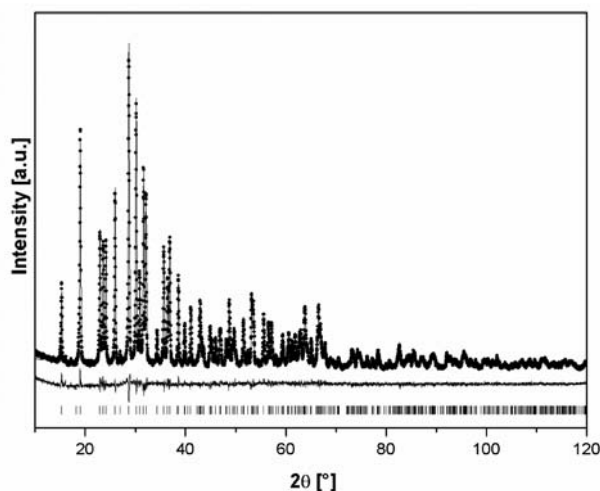


Figure 3. Final Rietveld plot of the  $\text{CuWO}_4$  powder.

general crystallographic positions  $2i$  with local symmetry 1. The least squares refinement were made by varying 35 parameters: one parameter for the scale factor, one zero point, six lattice constants, four for the description of the background, 18 fractional ionic coordinates, three isotrop-

**Table 1.** The structure of  $\text{CuWO}_4$  with space group  $P\bar{1}$  and unit cell dimensions  $a = 4.70887(10)$  Å,  $b = 5.84412(12)$  Å,  $c = 4.88457(9)$  Å and  $\alpha = 91.65183(121)$ ,  $\beta = 92.50790(124)$ ,  $\gamma = 82.80525(118)$ .

Atom	Position	X( $\sigma(X)$ )	Y( $\sigma(Y)$ )	Z( $\sigma(Z)$ )	B( $\sigma(B)$ )
W	$2i$	0.02049(24)	0.17364(16)	0.25426(26)	0.57(2)
Cu	$2i$	0.49744(71)	0.65811(46)	0.24645(65)	1.03(6)
O(1)	$2i$	0.25241(210)	0.34472(126)	0.42174(192)	0.85(10)
O(2)	$2i$	0.20829(186)	0.87575(128)	0.43315(189)	0.85(10)
O(3)	$2i$	0.73701(219)	0.37421(138)	0.10117(195)	0.85(10)
O(4)	$2i$	0.78033(183)	0.90519(129)	0.04858(191)	0.85(10)

**Table 2.** Interatomic distances (Å) and bond angles (degrees) in  $\text{CuWO}_4$ . The standard deviations are in brackets.

CuO <sub>6</sub> octahedra					
Cu–O(2)	1.99(5)	O(1)–Cu–O(1)	85.7(18)	O(2)–Cu–O(4)	103.4(15)
–O(1)	1.97(5)	O(1)–Cu–O(2)	86.1(17)	O(3)–Cu–O(3)	81.5(17)
–O(3)	1.92(4)	O(1)–Cu–O(3)	77.9(17)	O(3)–Cu–O(4)	92.3(15)
–O(3)	2.00(4)	O(1)–Cu–O(3)	88.3(17)	O(3)–Cu–O(4)	93.4(16)
–O(4)	2.32(4)	O(1)–Cu–O(2)	89.0(19)	O(1)–Cu–O(4)	169.8(14)
–O(1)	2.29(4)	O(1)–Cu–O(3)	86.6(18)	O(1)–Cu–O(3)	167.6(16)
		O(1)–Cu–O(4)	90.7(17)	O(2)–Cu–O(3)	163.7(18)
		O(2)–Cu–O(3)	101.4(18)		
WO <sub>6</sub> octahedra					
W–O(1)	1.86(5)	O(1)–W–O(2)	96.7(18)	O(2)–W–O(4)	81.8(17)
–O(4)	1.83(4)	O(1)–W–O(2)	101(2)	O(3)–W–O(4)	86.8(15)
–O(3)	1.87(4)	O(1)–W–O(3)	101.7(18)	O(3)–W–O(4)	99.0(18)
–O(2)	1.91(5)	O(1)–W–O(4)	98.3(18)	O(4)–W–O(4)	77.2(15)
–O(2)	2.07(4)	O(2)–W–O(2)	72.3(18)	O(1)–W–O(4)	171.0(16)
–O(4)	2.22(3)	O(2)–W–O(4)	75.9(16)	O(2)–W–O(3)	156.4(18)
		O(2)–W–O(4)	92.8(17)	O(2)–W–O(4)	156.8(16)
		O(2)–W–O(3)	89.7(19)		

ic thermal displacement factors, microstrain and crystal size. The distortion in  $\text{CuWO}_4$  is mainly reflected in the deviation of  $\gamma$  from  $90^\circ$ . Although the synthesis was performed in the presence of huge excess of  $\text{Cu}^{2+}$  ions, no traces of any other crystalline phase were noticed in the sample due to thorough post-synthetic washing treatment.

Results of the final Rietveld refinements (the unit cell dimensions) are presented in Table 1 and the final Rietveld plot is depicted in Figure 3. The crystallite size and micro strain of the whole pattern are 27.58 nm and 0.005%, respectively. The structure of copper tungstate was refined down to the R-factor of 5.4%. Values of estimated standard deviations as well as reliability factors confirmed that these data are reliable and that structure was well refined. Based on the fixed and refined fraction coordinates of the ions, interatomic distances (metal-oxygen) as well as bond angles (at the metal atoms and the corresponding oxygen-oxygen separation) were determined in  $\text{CuWO}_4$  octahedrons and presented in Table 2 with their estimated standard deviations.  $\text{WO}_6$  octahedra are slightly distorted in wolframite with W-O distances ranging from 1.83 to 2.22 Å, while the  $\text{CuO}_6$  octahedra have a pseudo tetragonally elongated geometry with four planar Cu-O distances from 1.92 to 2.00 Å and two axial Cu-O distances around 2.3 Å. The obtained coordinates of  $\text{CuWO}_4$  are in good agreement with data reported by Kihlborg.<sup>25</sup>

The  $\text{CuWO}_4$  is an indirect band gap semiconductor. The most of the band gap energy data were obtained using optical measurements with  $\text{CuWO}_4$  single crystals.

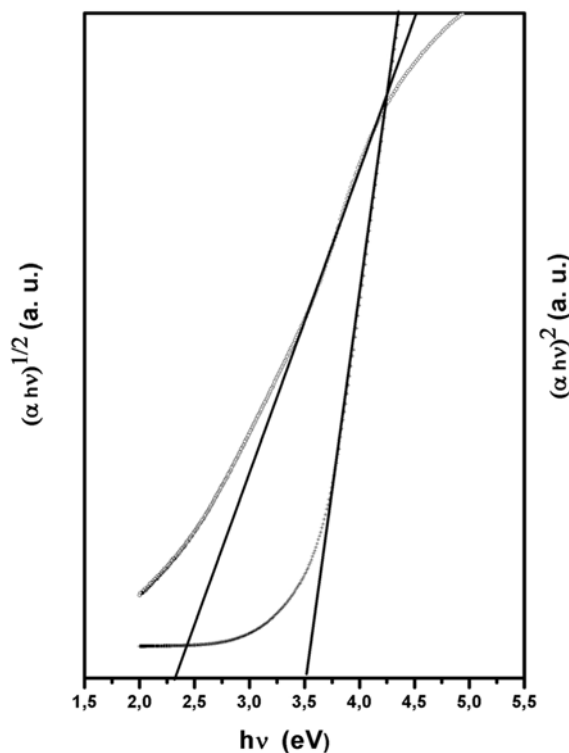


Figure 4. Tauc's plots for determination of band gap energies.

Two groups of data for direct band gap energy can be found in literature: 3.88 eV and much lower values in the range from 2 to 2.3 eV.<sup>8,26,27</sup> Recently, Pandey et al.<sup>28</sup> determined both, indirect and direct, band gap energies (1.9 and 2.1 eV, respectively) using  $\text{CuWO}_4$  thin films prepared from precursor synthesized by precipitation method and annealed in temperature range from 350 to 450 °C. Absorption spectra of colloids consisting of semiconductor nanoparticles that negligible scatter light are frequently used for band gap determination. In order to determine band gap energy, absorption spectrum of slightly turbid  $\text{CuWO}_4$  dispersion was analyzed using the following well-known relation:

$$\alpha = k(h\nu)^{-1}(h\nu - E_g)^{n/2} \quad (3)$$

where  $k$  is the constant,  $h\nu$  is the photon energy and  $n$  is equal to 1 for direct band gap and 4 for indirect band gap. Plots of  $(\alpha h\nu)^2$  and  $(\alpha h\nu)^{1/2}$  vs.  $(h\nu)$  for the  $\text{CuWO}_4$  are shown in Figure 4. As can be seen, both plots are linear. The values obtained by extrapolating the straight portion to energy axis at zero absorption coefficients gave the direct and indirect band gaps of 3.5 and 2.3 eV, respectively. The obtained band gap energy values are in reasonable agreement with already published data in literature.

To conclude, a new synthetic procedure for preparation of copper tungstate particles in nanometer size domain under mild experimental conditions was developed. Also, experimental conditions for preparation of  $\text{CuWO}_4$  without impurities were found and structural characterization was performed. Obtained material was optically characterized and direct and indirect band gap energies were determined. The extension of this approach for synthesis of other tungstate family members is under way in our laboratory.

## 4. Acknowledgments

Financial support for this study was granted by the Ministry of Science and Technological Development of the Republic of Serbia (Projects 172056, 45020 and 45015).

## 5. References

1. B. L. Chamberland, J. A. Kafalas, J. B. Goodenough, *Inorg. Chem.* **1977**, *16*, 44–46.
2. R. H. Gillette, *Rev. Sci. Instrum.* **1950**, *21*, 294–301.
3. L. G. VanUitert, S. T. Preziosi, *J. Appl. Phys.* **1962**, *33*, 2908–2909.
4. R. Bharati, R. Shanker, R. A. Singh, *Pramana*, **1980**, *14*, 449–454.
5. J. P. Doumerc, J. Hejtmanek, J. P. Chaminade, M. Pouchard, M. Krussanova, *Phys. Stat. Solidi (a)*, **1984**, *82*, 285–294.

6. L. G. VanUitert, R. B. Soden, *J. Appl. Phys.* **1960**, *31*, 328–330.
7. S. K. Arora, T. Mathew, N. M. Batra, *J. Crystal Growth*, **1988**, *88*, 379–382.
8. S. K. Arora, T. Mathew, N. M. Batra, *J. Phys. Chem. Solids*, **1989**, *50*, 665–668.
9. S. K. Arora, T. Mathew, *Phys. Stat. Solidi (a)*, **1989**, *116*, 405–413.
10. M. V. Šušić, Y. M. Solonin, *J. Mater. Sci.* **1988**, *23*, 267–271.
11. L. P. Dorfman, D. L. Houck, M. J. Scheithauer, J. N. Dann, H. O. Fassett, *J. Mater. Res.* **2001**, *16*, 1096–1102.
12. O. Y. Khyzhun, T. Strunskus, S. Cramm, Y. M. Solonin, *J. Alloys. Compd.* **2005**, *389*, 14–20.
13. S. M. Montemayor, A. F. Fuentes, *Ceramics International*, **2004**, *30*, 393–340.
14. E. Tomaszewicz, J. Typek, S. M. Kaczmarek, *J. Therm. Anal. Calorim.* **2009**, *98*, 409–421.
15. F. Zhang, M. Y. Sfeir, J. A. Misewich, S. S. Wong, *Chem. Mater.* **2008**, *20*, 5500–5512.
16. S. H. Yu, M. Antonietti, H. Colfen, M. Giersig, *Angew. Chem. Int. Ed.* **2002**, *41*, 2356–2360.
17. R. W. Cheary, A. A. Coelho, *J. Appl. Crystallogr.* **1992**, *25*, 109–121.
18. H. Rietveld, *J. Appl. Crystallogr.* **1969**, *2*, 65–71.
19. V. K. Pecharsky, P. Y. Zavalij, *Fundamentals of powder diffraction and structural characterization of materials*, Chapter 3 Springer, Berlin, **2005**.
20. Y. Li, S. Yu, *Int. Journal of Refractory Metals & Hard Materials*, **2008**, *26*, 540–548.
21. A. Sen, P. Pramanik, *J. Eur. Ceram. Soc.* **2001**, *21*, 745–750.
22. T. Montini, V. Gombac, A. Hameed, L. Felisari, G. Adami, P. Fornasiero, *Chem. Phys. Lett.* **2010**, *498*, 113–119.
23. K. Holmberg, *J. Coll. Int. Sci.* **2004**, *274*, 355–364.
24. M. Andersson, V. Alfredsson, P. Kjellin, A. E. C. Palmqvist, *Nano Letters*, **2002**, *2*, 1403–1407.
25. L. Kihlberg, E. Gebert, *Acta Cryst B*, **1970** *26*, 1020–1026.
26. M. Ch. Lux-Steiner, *Springer Proceedings in Physics, Polycrystalline Semiconductors II* **1991**, *54*, 420–431.
27. R. L. Perales, J. R. Fuertes, D. Errandonea, D. M. Garcia, A. Segura, *EPL*, **2008**, *83*, 37002–37007.
28. P. K. Pandey, N. S. Bhave, R. B. Kharat, *Electrochim Acta*, **2006**, *51*, 4659–4664.

## Povzetek

Bakrov volframat nanometrski velikosti smo sintetizirali z obarjalno metodo v prisotnosti površinsko aktivnega kopolimera in segrevanjem pri 400 °C. Z vrstično elektronsko mikroskopijo smo potrdili nastanek okroglih delcev velikosti med 10 nm in 90 nm. S termogravimetrično analizo smo spremljali proces dehidracije. Z rentgensko analizo smo potrdili nastanek triklinskega CuWO<sub>4</sub>. Prilaganje modela eksperimentalnim podatkom je potrdilo, da ima prah strukturo volframatnega tipa s prostorsko skupino P1. Strukturo lahko opišemo kot neskončne verige, sestavljene iz izmeničnih oktaedrov [W–O<sub>6</sub>] in [Cu–O<sub>6</sub>] s skupnimi robovi. Z optičnimi meritvami smo določili vrednosti energije prepovedanega pasu (2.3 in 3.5 eV).